COCCOLITH BIOMINERALISATION STUDIED WITH ATOMIC FORCE MICROSCOPY

by K. HENRIKSEN, J. R. YOUNG, P. R. BOWN *and* S. L. S. STIPP

ABSTRACT. Biomineralisation can only be understood as an interplay between organic and mineral phases. With this objective, we conducted an investigation of coccoliths using atomic force microscopy (AFM), an ultra-high resolution technique that requires no surface coating and can be used in air or under solution at ambient conditions of temperature and pressure. The detailed morphology, crystal structure, organic scales and organic coating of the coccolith species *Coccolithus pelagicus*, *Helicosphaera carteri* and *Oolithotus fragilis* were investigated. The fine structure of coccoliths is very complex, with the calcite either being smooth, dominated by steps or tuberculate; organic cover can be either granular or fibrous. Behaviour of coccolith surfaces during dissolution is influenced both by mineral and organic material and different surface types show variable resistance to dissolution. The organic coating protects element faces against etching. Through atomic resolution AFM, it is possible to establish the crystallographic structure of the distal shields of *C. pelagicus* and *O. fragilis*. Though elements of both species are dominated by stable crystal faces, there are important differences between them, with the external edge of elements being parallel to a cleavage direction in *C. pelagicus* but parallel to the atomic rows in *O. fragilis*. Thus, there is evidence that the biomineralisation of each species, and also of select areas of coccoliths of the same species, is markedly different.

KEY WORDS: biomineralization, coccolithophores, AFM, dissolution pattern, calcite.

THE science of palaeontology relies primarily on the fossilised hard-parts of organisms, the products of a series of processes collectively known as biomineralisation. The mechanisms of biomineralisation direct the composition, crystallographic structure and morphology of the biominerals; any change in these is a reflection of an alteration of the underlying process. In palaeontology, the importance of morphological change through time can hardly be exaggerated and therefore, understanding the factors that control biomineralisation is essential. This focus on process as well as product is necessary, because there are cases where a relatively trivial change in the mineralisation process produces a relatively large morphological output (Young and Henriksen, 2003).

Biomineralisation occurs in all types of organisms from bacteria to vertebrates and from unicellular algae to higher plants. It results in both amorphous and crystalline materials, with oxides, silica and carbonates being common. The control exerted by the organism ranges across a spectrum from biologically induced biomineralisation, where precipitation occurs extracellularly as a by-product of the metabolic activity of the organism, to biologically controlled mineralisation, where composition, crystallographic structure and morphology is completely regulated (Mann 1983). End products of biologically controlled biomineralisation reach a strength, flexibility and complexity that is far superior to materials that can be manufactured in the laboratory (Mann 1993).

Coccolithophores are examples of relatively simple organisms that produce startlingly complex biominerals, the coccoliths. These are divided into two fundamentally different kinds: holococcoliths and heterococcoliths (Braarud *et al.* 1955; Young *et al.* 1999). The holococcoliths consist of a large number of miniscule, equant calcite crystals held together by organic material and are only rarely preserved in the fossil record. Heterococcoliths consist of fewer calcite crystals ('crystal units') of complex shape that mechanically interlock along crystallographically controlled edges, giving much higher preservation potential. In this group, biomineralisation has been studied extensively both by biochemists as an accessible test group to probe the fundamental controls on biomineralisation and by

[Palaeontology, Vol. 47, Part 3, 2004, pp. 725–743, 5 pls]

taxonomists interested in elucidating the phylogeny of the group. It has been shown that although coccoliths vary greatly in morphology and appearance under a light microscope, the basic mechanism in their construction is the same (Young *et al.* 1992, 1999). This mechanism produces the pattern of nucleation of the crystal elements that make up the coccolith. Nucleation is believed to occur on an organic template, which leads to crystallographic control of the nucleating calcite, presumably by presenting a motif of charge distribution with a spacing that corresponds to a certain face of the crystal, which is then selectively developed as the compounds of the mineral attach to the available binding sites (Young *et al.* 1999). Coccoliths grow from a proto-coccolith ring of crystals having their *c*-axes alternately oriented approximately radially ('R units') and vertically ('V units') relative to the plane of the coccolith (Young *et al.* 1992). This V/R nucleating pattern has been documented for both living and fossil genera and has been conserved within the heterococcoliths through the 230 myr span of their fossil record. In *Emiliania*, the V units are relict structures that do not develop beyond the earliest proto crystals and are quickly overgrown by the R units. Thus, even for species that appear to consist of crystals in a single orientation, the pattern of nucleation remains the same (Young *et al.* 1992).

Biomineralisation of heterococcoliths is a wholly intracellular process. It occurs in a vesicle derived from the Golgi-body ('the coccolith vesicle'), on an organic scale known as a base-plate scale to which the template is presumably attached. The base-plate scale stays with the coccolith. The chemical composition of the fluid in the coccolith vesicle is isolated from the cytoplasm, and supersaturation of calcite is achieved through the action of acidic polysaccharide complexes with calcium ('coccolithosomes') that are transported into the vesicle (documented for *Pleurochrysis carterae*; Outka and Williams 1971; van der Wal *et al.* 1983; Marsh 1994). Once stable calcite nuclei have formed, the morphology of the crystals is tightly regulated so that they intergrow to give the complex shape of a coccolith. The strict morphological control is the most enigmatic part of biomineralisation; it is probably brought about by a combination of organic inhibitors of crystal growth and mechanical stresses applied by the coccolith vesicle (Young *et al.* 1999). When growth is complete, remaining coccolithosomes disaggregate and the organic species bind to the crystals, forming a coating that stays with the coccolith (Marsh 1994). Then the coccolith is transported to the exterior of the cell through exocytosis.

It is the interplay of organic material with inorganic crystals that facilitates the large range of morphologies possible in biominerals and allows organisms to produce materials that are both stronger and more flexible than their purely inorganic counterparts. Thus, understanding biomineralisation is only possible through investigating both biocrystals and the organic material associated with them. Therefore, we have conducted an investigation of the crystal structure and morphology of coccoliths and the nature of their organic coating. This has been done using atomic force microscopy (AFM), a technique that can image the surface of a relatively flat sample with resolution several orders of magnitude higher than is possible with optical or scanning electron microscopy (SEM). Under the right conditions, AFM can resolve the atomic structure of the sample. Atomic force microscopy has previously proven useful in biomineralization research (e.g. Smith *et al.* 2000; Crawford *et al.* 2001; Orme *et al.* 2001), and there are several reasons why AFM of coccoliths is an attractive approach to study their biomineralization: (1) The technique can be used *in situ*, requiring no coating of the sample or the use of ultra-high vacuum; it works well under normal conditions of temperature and pressure, and samples can be imaged in air or solution. (2) Because of the lack of coating, AFM is dynamic. The surface is imaged as changes occur, for example during precipitation and dissolution. (3) Using AFM, it is possible to obtain accurate distances in the vertical dimension, so that the true heights of features can be determined with resolution on the order of 1/10 Ångström (10^{-11} m).

During the course of this study, the advantages offered by AFM allowed investigation at high resolution of structure and morphology of three heterococcolith species: *Coccolithus pelagicus*, *Helicosphaera carteri* and *Oolithotus fragilis*. We observed behaviour during dissolution and investigated the nature and influence of the organic coating by comparing samples before and after treatment to remove it by oxidation. For comparative purposes, we also imaged the samples with scanning electron microscopy (SEM), the traditional technique in coccolith ultrastructure research, but using a high resolution Field Emission SEM to obtain images of high quality.

STRUCTURE OF *COCCOLITHUS PELAGICUS*, *OOLITHOTUS FRAGILIS* AND *HELICOSPHAERA CARTERI*

Coccolithus pelagicus coccoliths are elliptical placoliths with 30–60 elements per cycle, typically possessing a central opening that may be spanned by a bar (Pl. 1, figs 1–2) (Young 1993). It has an organic base-plate, which is patternless except for a slight thickening at the margin, and small oval scales with radial and concentric fibrils (Manton and Leedale, 1969; Billard 1994). The bar is the only part of the coccoliths that is not formed by the V and R elements of the proto-coccolith ring. In *C. pelagicus*, the V units form the distal shield (which consequently appears dark in cross-polarised light) and the lower tube elements, whereas the R units form the proximal shield, which is two-layered, and the upper tube elements (Pl. 1, fig. 3). The zone of intergrowth, which is the locus of the original proto-coccolith ring, is situated above the base of the coccolith, between the shield and tube elements. This means that growth of the elements occurs upwards, inwards, outwards and notably also downwards from the original nuclei; thus, the base-plate scale does not block downward growth (Young 1993). Two morphotypes of *C. pelagicus*, a small subarctic and a large temperate form, are now recognised (Baumann *et al.* 2000). There is evidence that these are in fact separate species (Geisen *et al.* 2002). In this study, all culture material used was of the large *C. pelagicus*.

Oolithotus fragilis coccoliths are circular to subcircular placoliths with 18–20 elements in the shield, crenulate periphery, a circular central area, somewhat offset from the middle of the distal shield, with no central opening (Pl. 1, figs 4–5) (Kleijne 1993). The proximal shield is significantly smaller than the distal shield. The V/R structure of *O. fragilis* is relatively simple, having a distal shield composed of V units and a proximal shield of R units (Pl. 1, fig. 6) (Young *et al.* 1992). As in *Coccolithus*, growth occurs downward from the proto-coccolith ring as well as upwards, so that in the mature coccolith, the locus of the proto-coccolith ring is embedded within the coccolith tube.

Helicosphaera carteri coccoliths are symmetrically to asymmetrically elliptical and the distal shield has a spiral morphology, so that there is a zone of overlap where the distal shield is double (Pl. 1, figs 7–8). The proximal shield (also known as the base-plate) has a principal suture or two narrow central openings separated by a bar. Covering the distal central area and extending out over the shield elements is a blanket of superimposed laths (Theodoridis 1984). The distal and proximal shields are made up of V units whereas the blanket and central area are formed by the R units (Pl. 1, fig. 9). Plate 1, figure 10 shows where the two types of element join on the proximal face. Careful SEM observations of specimens in various states of preservation reveal that the apparent multitude of laths in the blanket are in fact not separate crystals but rather surface features on the R units formed by numerous steps (Pl. 1, fig. 11).

ATOMIC FORCE MICROSCOPY

Microscopes with the ability to image surfaces with resolution of a few Ångströms (10^{-10} m) were first invented in 1982 (Binnig *et al.* 1982*a*, *b*), and have had a tremendous impact in many branches of science including physics, chemistry and materials science. These microscopes all belong to a family of techniques known as scanning probe microscopy (SPM), and are based on the interaction of a sharp tip with the surface of a sample. Images are generated by rastering the sample beneath the tip in multiple parallel lines. The techniques differ in choice of probe and which physical parameter is measured as the sample moves beneath the tip. The key to the high resolution of SPM is the ability to control accurately very minute movements of the sample, so that the area scanned is very small. This is achieved by a scanner of piezo-electric ceramic characterised by its ability to bend slightly in response to a voltage. Very small voltages move the ceramic, upon which the sample is mounted, only fractions of a nanometre at a time. The atomic force microscope (AFM; Binning *et al.* 1986) measures the forces acting between tip and surface, by monitoring the amount of deflection on the tip, which is mounted on a triangular cantilever with a very low spring constant (Text-fig. 1A). Because the measurement of forces can be atomically local, it is possible to make true atomic resolution images with AFM when the conditions are right (Ohnesorge and Binnig 1993). Commonly, two types of image can be obtained simultaneously during AFM imaging: a height image and a deflection image; this is possible because every line is scanned twice (back and forth). Height images give true information about distances in z, but if a sample is relatively rough, this means that fine

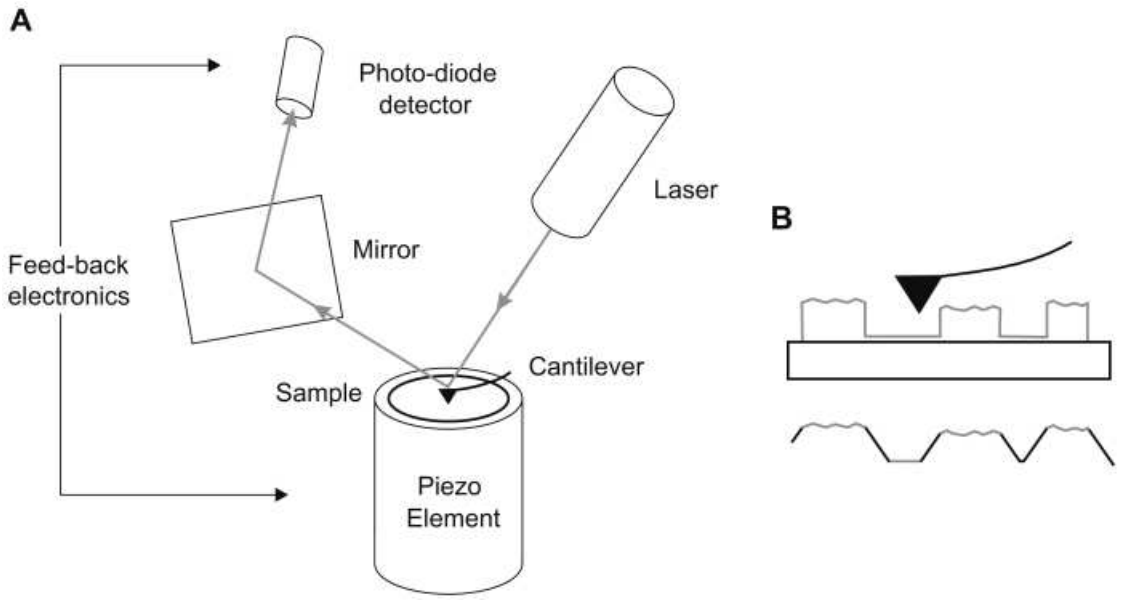

TEXT-FIG. 1. A, atomic force microscopy. The sample is mounted on a piezo-ceramic element that rasters it beneath a sharp cantilever. A laser is shone on the back of the cantilever, and a position-sensitve detector records the amount of deflection on the tip. Very fast feed-back electronics allow adjustment of the sample position in response to the deflection. B, generation of tip-artefact. A sample (grey) is scanned by the tip; when surface features are steeper than the curvature of the tip, the shape of the tip is recorded. The recorded morphology is shown below; areas of tip-artefact shown in black.

structure will not be recorded. Deflection images can record fine structure on rough samples, but give no true heights, which is why it is so useful to obtain both types of image at once.

AFM of calcite

Earlier studies (Stipp *et al*. 1994; Stipp 1999) of calcite crystals have revealed the atomic scale topography of the hydrated rhombic $(10\bar{1}4)$ surface. It is characterised by a surface unit cell of 5×8 Å, and a characteristic pairing of rows as well as an alternation of slightly higher and lower points along the atomic rows (direction of minimum inter-atomic distance). Therefore, the rhombic face can be recognised, its orientation in three dimensions determined, and by identifying the atomic row direction, the crystallographic orientation of the mineral is found. In this way, the AFM is capable of revealing the c-axis direction and the orientation of the a-axes, completely resolving the crystal orientation.

EXPLANATION OF PLATE 1

Figs 1–3. *Coccolithus pelagicus*. 1, SEM of coccosphere. 2, SEM of coccolith. 3, V/R structure with V units in grey and R units in black. Position of base-plate scale is indicated.

Figs 4–6. *Oolithotus fragilis*. 4, SEM of coccosphere. 5, SEM of coccolith. 6, V/R structure, colour coding as in 3.

Figs 7–11. *Helicosphera carteri*. 7, SEM of coccosphere. 8, SEM of coccolith. 9, V/R structure, colour coding as in 3. 10, SEM showing how V and R units join on the proximal face. 11, SEM of a slightly etched specimen showing that the blanket is composed of few elements of complex morphology rather than a multitude of individual laths.

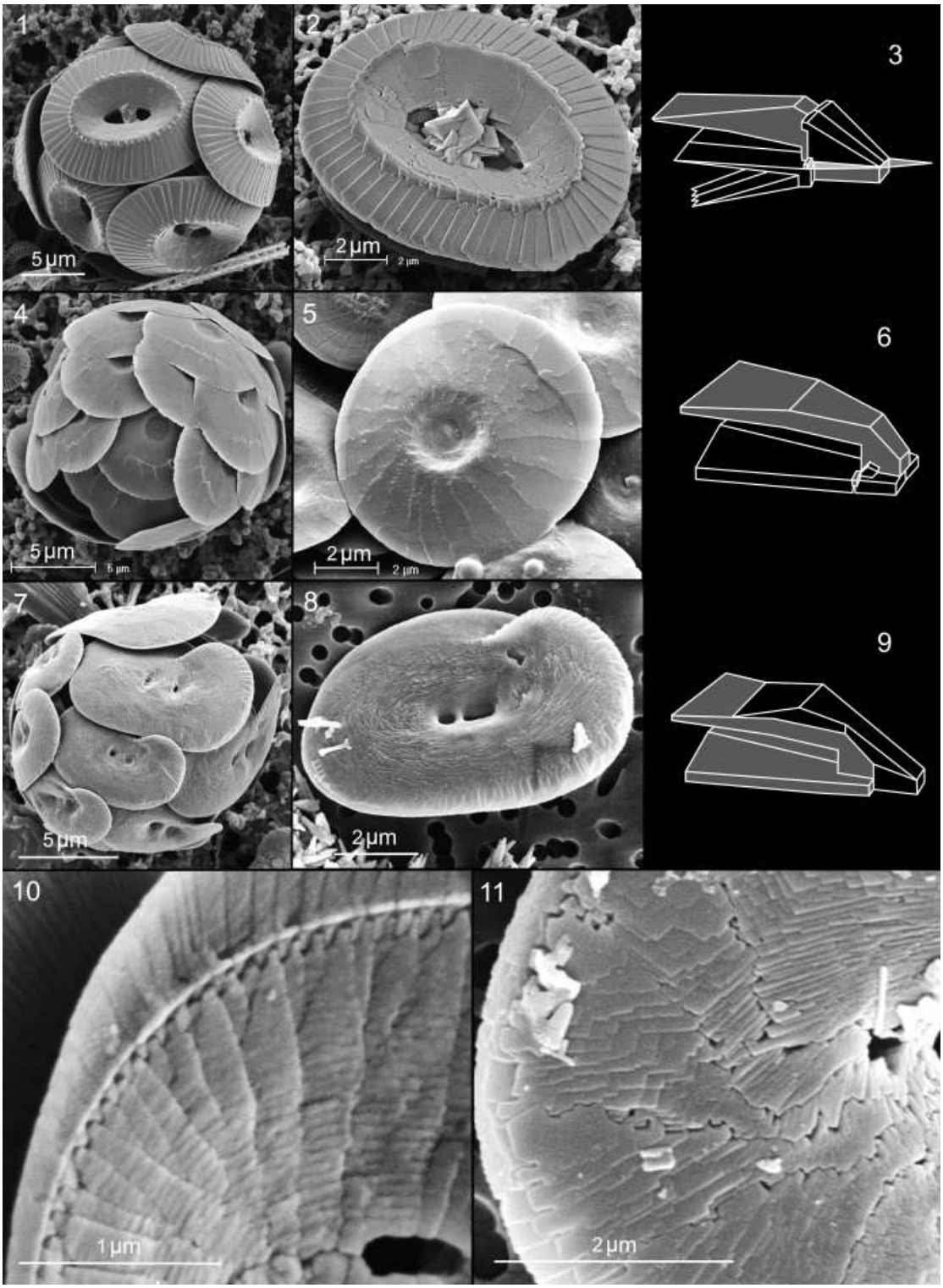

HENRIKSEN *et al.*, coccolith biomineralisation

Artefacts

There are several ways in which the features shown on AFM images may deviate from what is actually present on the sample. One way this can happen is if the area scanned by the tip is not of the exact size and shape that is intended; when shown on the image, the data are presented as if the intended scan had been performed, so the features of the image are distorted. This distortion must be taken into account when very accurate distances and angles have to be obtained (Henriksen and Stipp 2002).

Another set of imaging artefacts is caused by the nature and topography of the tip. Standard AFM tips are pyramidal and the imaging point has a radius of curvature of about 50 nm. Problems arise when trying to image surfaces that have sharper relief than the tip curvature; in these cases the shape of the tip rather than that of the surface feature is recorded. This produces images with very characteristic artefacts because the morphology of the tip is easy to recognise. Text-figure 1B shows how the AFM image represents a convolution of the tip and surface shapes. For a general review of the AFM imaging process and possible artefacts, see Eggleston (1994).

EXPERIMENTAL STRATEGY AND DETAILS

All studies were based on monoalgal coccolithophore clones grown in The Natural History Museum, London and the University of Caen. The advantage of using culture material, rather than fossil or filter samples, is that these cultures are monospecific, and alive or recently dead at the time of sample preparation, so that the calcite and organic cover are pristine. With the atomic force microscope, samples were imaged in air, under buffered solution and while subjected to gradual dissolution. These experiments were performed on both untreated coccoliths and material where the organic coating had been removed by oxidation. A scanning electron microscopy investigation of the culture samples used in the AFM study was also undertaken.

Scanning electron microscopy

The SEM investigations were carried out on a Philips XL-30 FEG field emission scanning electron microscope. Samples were prepared by pipetting a droplet of suspended coccoliths onto a polycarbonate (millipore) or cellulose nitrate filter with a pore size of 0·44–0·8 μm overlying an absorbant pad. When the moisture had drained through, the filter was cut and mounted on a piece of photographic film glued to an SEM stub. Samples were sputter-coated with a 20 nm layer of gold/iridium.

Atomic force microscopy

The AFM experiments were conducted using a Digital Instruments Multimode SPM running in Contact AFM mode. In order to minimise vibration transmitted through air and building, the instrument could be hung on a platform suspended on rubber cords from the ceiling and covered with hoods of aluminum and foam. For this study, a piezo-electric scanner with maximum x and y offsets of about 13 μm was used. Probes were standard, commercially available pyramidal tips of Si_3N_4 integrated on a gold-coated cantilever with a spring constant of about 0·6 nN. A glass fluid cell was used with the O-ring removed in order to enable easier movement of the sample for selection of imaging area. During imaging, force on the tip was minimised by lowering the zero-point on the photosensitive detector. Since the distortion in AFM that influences angular relationships decreases with operation time (Henriksen and Stipp 2002), we used only images taken after at least 70 minutes for measuring angles.

For imaging in air, coccoliths were attached to a sample holder using either freshly cleaved HOPG (highly ordered pyrolytic graphite) or mica coated with the long-chained polymer polyethyleneimine (PEI). The graphite was cleaved using a piece of double-adhesive tape, which was then mounted on the sample holder, and a droplet of solution containing suspended coccoliths was pipetted onto the surface. The moisture was sucked away using a piece of tissue. PEI coated mica was prepared following the method described by Bosbach *et al.* (2000) and a thin spread of coccoliths was attached to it using the same procedure as for graphite. For fluid-cell imaging, coccoliths were mechanically pressed into a piece of

malleable foil. This method has the disadvantage of causing breakage of the specimens, so that whole coccoliths rarely can be imaged.

Dissolution experiments

Coccoliths were imaged in the fluidcell under a solution of 0·05 M NH_4HCO_3, a buffer that ensures surface stability. Subsequently, gradual surface dissolution of samples was induced by adding droplets of deionized water (pH = 5·6) onto the surface. When a droplet was put on the sample, equilibrium with the surface was attained very quickly (< 1–2 minutes), indicated by etching features being present but stable when the first image could be taken. Sucking away the equilibrated fluid and adding a new water droplet caused further etching, and repetition of this procedure yielded a series of snapshots of the same surface in progressive states of dissolution. No specimens could be observed throughout the entire dissolution sequence, because etching caused them to become too small for their depression in the foil whereupon the tip dislodged them.

Treatment for removal of organic coating

The layer of acidic polysaccharides that coat the coccoliths was removed by oxidation in a 1:1 mixture of 1N NaOH and concentrated NaOCl (15%) for 5 hours or overnight. To test whether this strongly alkaline solution causes dissolution of calcite, an investigation of its interaction with the surface of calcite crystals of high purity ('Iceland spar') was carried out. AFM images of Iceland spar treated with the oxidising solution alone showed clear signs of etching, whereas no dissolution could be observed when the liquid had been equilibrated with calcium carbonate before use. Therefore, the oxidising solution was always equilibrated with calcium carbonate before the coccoliths were exposed to it.

RESULTS

Good quality AFM images of coccoliths were obtained over the whole range of *E*-scanner sample areas, from 13 μm maps of whole specimens to nanometre scale images with atomic resolution. The surfaces of untreated coccoliths were found to be non-dynamic both in air and solution where no dissolution or precipitation was observed. The vertical drops at the edges of coccoliths invariably produce a tip artefact, which is unavoidable but easily recognisable.

Coccolithus pelagicus *imaged in air*

Plate 2, figures 1–3 show the distal surface of *C. pelagicus*. The distal shield elements are laths about 2 μm long. Their surface is covered with rounded bumps, giving a granular texture (Pl. 2, figs 2–3). In addition to this surface ornament, AFM of *C. pelagicus* shows the presence of vertical steps on some elements, most commonly parallel to the external edge (arrow on Pl. 2, fig. 2). The distal central area of *C. pelagicus* consists of numerous rhombic laths from 200 nm–1·5 μm in length, imbricated in a spiraling pattern. They are covered by bumps of similar morphology to those of the shield elements, but somewhat smaller. Curved vertical steps are present on the laths.

Proximal shield elements have a much more irregular outline than those of the distal shield, generally bifurcating twice towards the external edge (Pl. 2, figs 4–5). They show a granular surface texture, more pronounced than that of the distal surface, and vertical steps that tend to be straight and parallel to the external edge of the shield. Tubercles are observed on the proximal side of the distal shield (Pl. 5, fig. 5).

The proximal central area consists of a large number of imbricated crystals. On some specimens, the central pore was 'plugged' by a flat surface, approximately 130 nm below the plane of the innermost elements of the central area (Pl. 2, fig. 4). This surface is also recognisable on SEM images in both distal and proximal views (Pl. 5, fig. 11) and is probably the organic base-plate scale of the coccolith. Rather remarkably, this scale does not underlie the coccolith, as predicted by e.g. Manton and Leedale (1969), but lies part way up the central tube and appears to pass into the cocccolith. Elliptical scales approximately

2 μm across, displaying a microfibrillar structure of concentric ellipses and radially projecting lines, are often observed on the proximal surface (Pl. 2, figs 5–6). They are body scales of the coccolithophore.

Dissolution of C. pelagicus

Gradual dissolution of distal shield elements results in the formation of dissolution fronts (Pl. 2, figs 7–9). Initial dissolution rounds the edges of the elements and progresses inwards, forming rounded incisions. Faces dissolve as crystal fronts retreat parallel to element edges. Corners are round where edges meet. Dissolution enhances features initially present in a crystal, so the emergence of layers hints at slightly inhomogeneous conditions during formation. At advanced stages of dissolution, resistant islands appear on the faces. These areas are rounded and located predominantly near the element edges (Pl. 2, fig. 9).

C. pelagicus *after oxidising treatment*

After oxidation, *C. pelagicus* coccoliths were imaged in the fluid cell. Two surface textures are present: either coccoliths are very smooth or covered by a granular layer similar to the one observed on untreated specimens. Images showing the atomic pattern were obtained on the distal shield of a smooth specimen (Pl. 4, figs 2–3) (see crystallographic information section).

Dissolution of C. pelagicus *after oxidising treatment*

Coccoliths subjected to oxidation behave differently from untreated ones during dissolution (Pl. 2, figs 10–12). On elements of the distal shield, initial dissolution occurs in etch pits and along dissolution fronts over the whole of the faces. Edge morphology is very regular, corresponding to a rhombic pattern. The deep incisions in edges that are observed on untreated samples are not present. Advanced dissolution produces rounded rhombohedral hillocks. In general, samples treated to remove organic coatings dissolve on faces to a much larger extent than untreated samples.

Oolithotus fragilis *imaged in air*

The distal shield of *O. fragilis* (Pl. 3, fig. 1) is subcircular and consists of about 20 elements that run from the central area to the rim. The sutures are curved in the central area. The shield surface is divided into inner and outer zones with different suture patterns and surface characteristics. In the outer zone, the sutures are straight and the elements' surfaces are planar. In this area the faces appear coarsely granular at high magnification in the AFM. In the inner part of the shield the sutures show complex meandering patterns and the element surface is broken by a series of steps which imparts a new angle to the element surface (Pl. 3, figs 1, 3, 7). In this area the granular texture is less pronounced and curved fibres several micrometres long lie on the surface and cross suture lines.

The proximal shield of *O. fragilis* consists of 15–20 elements divided by incised, jagged sutures (Pl. 3,

---

EXPLANATION OF PLATE 2

Figs 1–6. AFM of *Coccolithus pelagicus*. 1, distal shield. 2, distal shield elements showing granular surface texture and steps (arrow). 3, granular surface texture. 4, proximal shield showing base plate scale. 5, proximal shield covered in body scales. 6, body scale.

Figs 7–9. AFM of *C. pelagicus* distal elements undergoing dissolution. 7, specimen before etching. 8, incisions form in edges and edge-parallel crystal fronts retreat across the elements. 9, rounded, dissolution resistant islands form on the elements.

Figs 10–12. AFM of *C. pelagicus* distal elements without organic cover undergoing dissolution. 10, specimen before etching. 11, etch pits form on the faces close to the edges. 12, large, broad etch pits form on the faces and dissolution-resistant islands stand out. The behaviour of the surface is very regular, conforming to the rhombic calcite pattern.

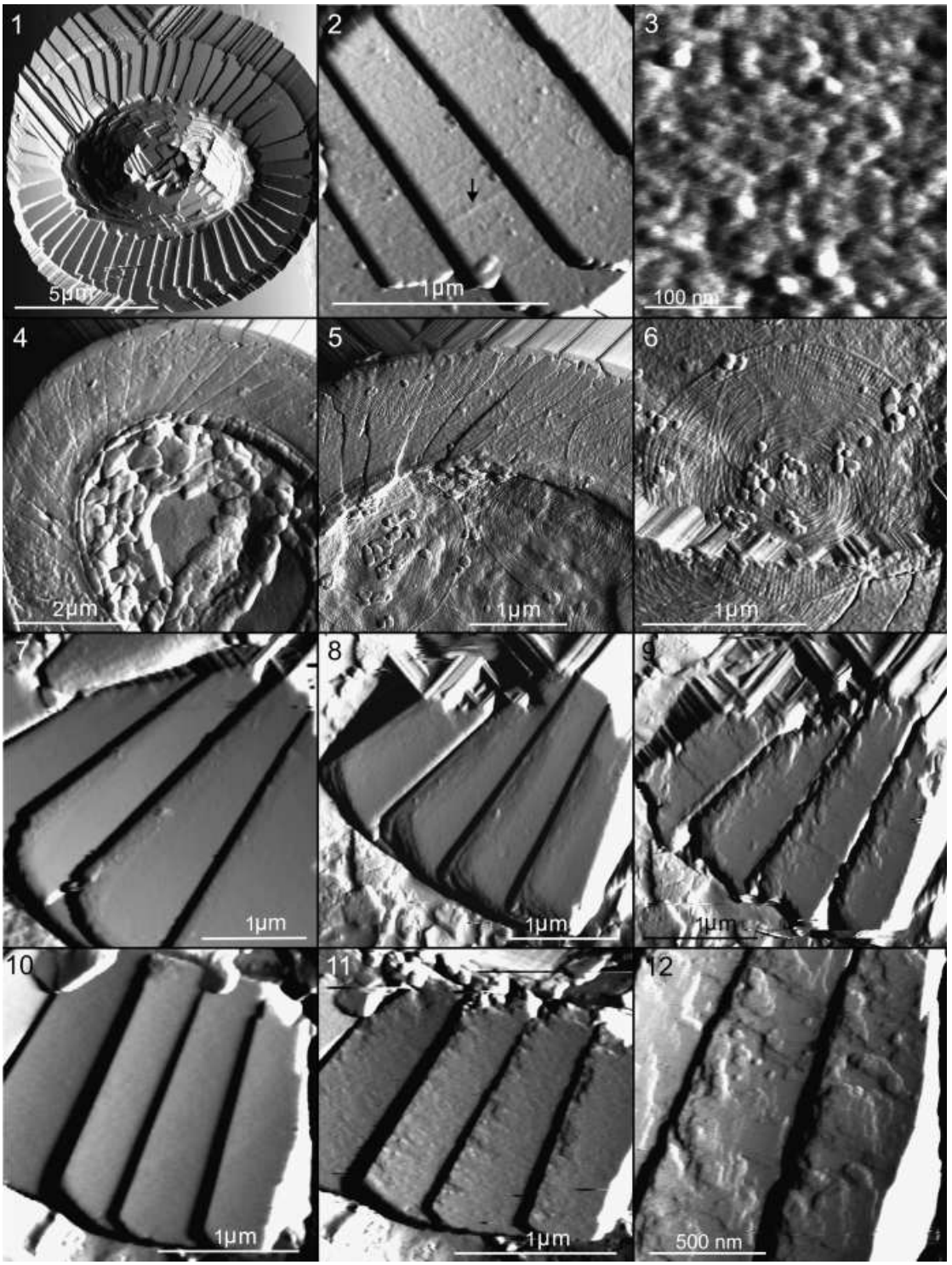

HENRIKSEN *et al.*, coccolith biomineralisation

fig. 2). The surface texture is granular with no sign of the fibrous ornament seen on the distal shield. Steps parallel to the outer edge are common. The underside of the distal shield is irregular and covered in large low bumps. Near the sutures, this texture thickens to form suture-parallel ridges.

Dissolution of O. fragilis

Gradual dissolution of an *O. fragilis* distal shield element (Pl. 3, figs 4–6) first occurs by formation of incisions in the sutures and external edge. Subsequently, irregular etch pits develop on the face, growing progressively wider and deeper. Pit shapes are irregular but the outer edge follows the vertical steps that run parallel to the edge of the element. Rounded areas stand up from the bottom of pits, and grow taller with increasing dissolution.

O. fragilis *after oxidising treatment*

We obtained images of atomic structure on the outer part of the distal shield of oxidised *O. fragilis* (Pl. 3, fig. 8), allowing us to interpret element crystallographic orientation. The underside of this shield (Pl. 5, fig. 4) shows a tuberculate texture. Tubercles appear arranged in rows parallel to the outer edge of the element, and the surface between them is covered in smaller bumps. The proximal shield shows a granular surface texture. The areas close to the sutures are raised in ridges.

Helicosphaera carteri *imaged in air*

The distal surface of *H. carteri* (Pl. 4, fig. 7) is almost completely covered by a blanket of laths, so that only a few of the distal shield elements are visible. These are about 1 μm in length; they have straight edges and a granular surface texture. The distal blanket consists of complex outgrowths from the R units resembling a larger number of stacked laths that are approximately 0·5 μm long (Pl. 4, fig. 8). Lath-shape is commonly rhombic, modified by kinks.

The proximal shield is almost invariably covered by organic material that obscures the elements (compare Pl. 4, fig. 9 with Pl. 1, fig. 10) and extends across the central openings. The organic cover is divided into an outer zone with fine radial, microfibrillar structure and an inner zone with an irregular, coarser fibrous texture. This cover is almost certainly the base-plate scale of the coccolith.

Crystallographic information

AFM allows determination of the crystallographic structure and observation of the behaviour of the organically grown coccolith calcite. Images with atomic resolution show the relation of distal shield elements of *C. pelagicus* and *O. fragilis* to the calcite cleavage rhomb (Pl. 3, fig. 7; Pl. 4, fig. 6). In both cases, they reveal a pattern corresponding to the rhombic '*r*' face of calcite, with surface unit cell dimensions of approximately 5×8 Å known from pure inorganic crystals (Stipp *et al.* 1994; Stipp 1999). In

---

EXPLANATION OF PLATE 3

Figs 1–3. AFM of *Oolithotus fragilis*. 1, distal shield. 2, proximal shield. 3, close-up of distal shield element showing granular and fibrous surface type.

Figs 4–6. AFM of *O. fragilis* distal element undergoing dissolution. 4, specimen before etching. 5, incisions form in edges and etch pits develop on the areas broken by numerous steps. 6, etch pits grow deeper and wider.

Fig. 7. A, the relation of a schematic element of *O. fragilis* to the calcite cleavage rhomb. B, schematic cross-section through the rhomb showing element profile.

Fig. 8. AFM image showing atomic structure on a distal shield element of *O. fragilis*.

Fig. 9. Distal element *O. fragilis*. Kinks in sutures seem to follow cleavage directions (black), but the outer termination is parallel to the atomic rows (dashed line).

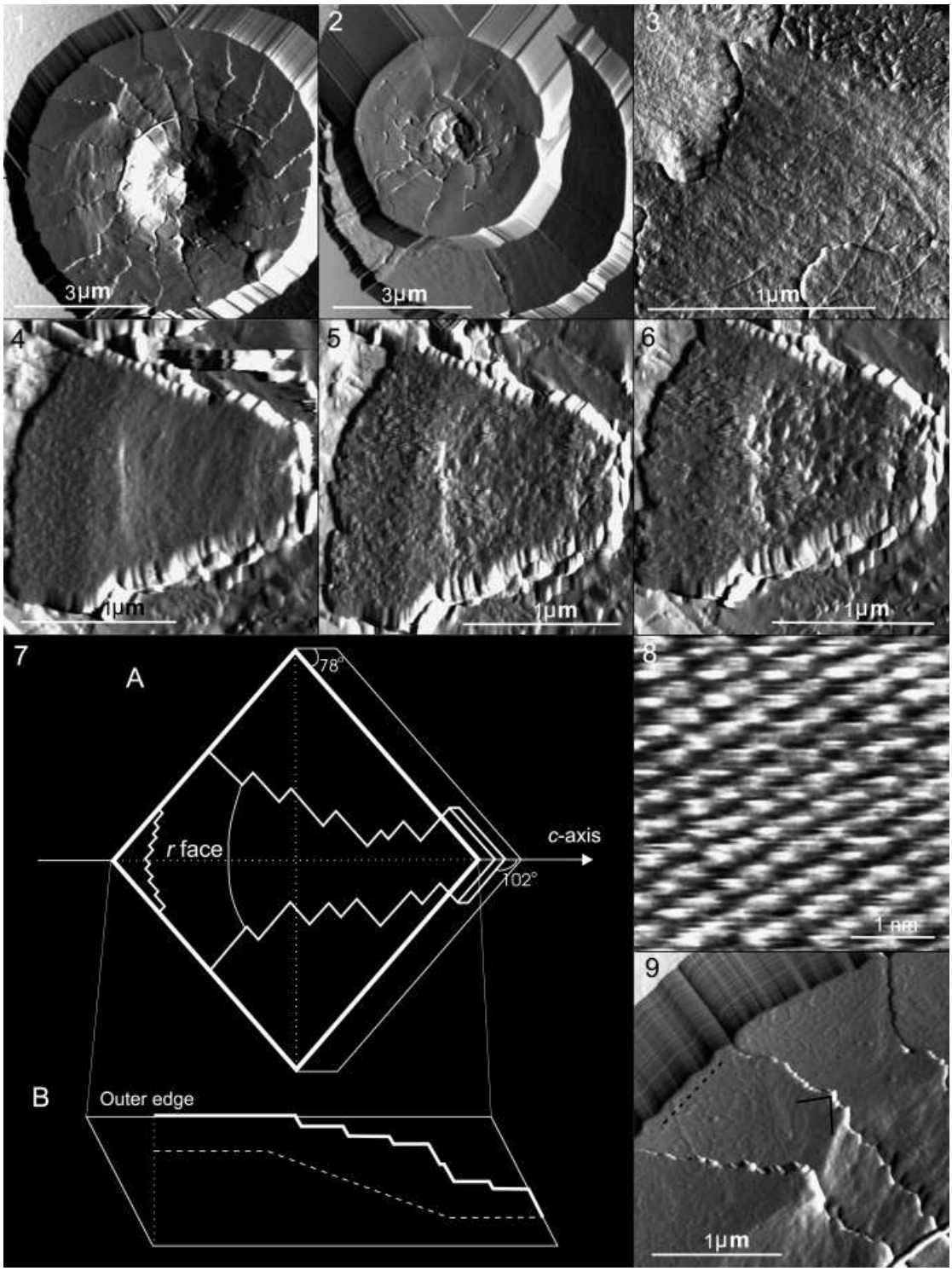

HENRIKSEN *et al.*, coccolith biomineralisation

addition, the atomic structure images reveal the specific orientation of the *r* face, so that crystallographic directions on the element surface are determined. Images at lower magnification, and cross-sections derived from them, show the angular relationships between the face and its edges, allowing us to interpret the relation of element edges to calcite cleavage. For *C. pelagicus*, the distal elements are rhombs bound by cleavage surfaces on the distal side as well as the outer and radial edges. Specimens of *O. fragilis* show much greater modification of the rhombic motif, with only the flat, outer parts of elements being smooth rhombic faces. Towards the centre, numerous steps and terraces give the elements their curvature down towards the middle of the coccolith. The radial edges of elements contain many kinks at angles corresponding to calcite cleavage, whereas the outer edges are modified by a series of kinks to follow a direction parallel to that of the atomic rows. Further details of the atomic structure study and their implications are presented in Henriksen *et al.* (2003).

Scanning electron microscopy

The cultures used for imaging with AFM were investigated with SEM to gain a general overview. The material was well preserved and only few examples of malformation were observed (Pl. 5, figs 1–2).

High resolution scanning electron micrographs of coccoliths commonly show a surface texture that is not smooth, and at first glance resembles the granular texture observed with AFM. However, examination of the filter substrate revealed a similar granular texture, which must be an artefact of sample preparation. Possible causes of the artefact include material precipitating or falling out of suspension as well as the metal sputter coating covering the SEM samples. To test the nature of the artefact and establish whether it is a feature that could also influence AFM imaging, a close scrutiny of coccolith surface features and a series of blank samples was undertaken with SEM. Surface textures of three types were found:

1. Tubercles that are a part of the coccolith calcite structure, as those seen on the proximal side of distal shields (Pl. 5, fig. 3). In SEM they are present while the proximal shield shows no similar surface texture; this non-uniformity of texture precludes them being an artefact of preparation. AFM images of coccoliths after exposure to oxidising solution also show tubercles on the underside of distal shields, suggesting that they are part of the calcite structure of the elements.
2. Granular surface texture which is probably formed by the organic cover of the coccoliths. This is seen to drape across sutures and cover whole coccoliths but is not similar to the texture of the SEM substrate, and thus is not an artefact (Pl. 5, figs 6–7). Commonly, AFM images of coccoliths with organic coating show similar granular surface textures.
3. Artefact of SEM preparation. This granular texture, which resembles the two mentioned above, covers both coccoliths and substrate (Pl. 5, figs 8–9). It is also present on filters that have only been exposed to water (Pl. 5, fig. 10) and, therefore, cannot be caused by organic material from the coccolith samples (which would also influence AFM imaging). Its source is probably the organic material on the photographic film used to mount the samples.

EXPLANATION OF PLATE 4

Figs 1–3. AFM images progressively zooming in on distal elements of *C. pelagicus* without organic coating. White squares give the position of the subsequent zoom. 2–3 show the atomic lattice (somewhat distorted).

Figs 4–5. AFM of *C. pelagicus*. Edges of elements and steps are often parallel to cleavage directions (black), but other directions, including parallel to the atomic rows (dashed line), are developed as well.

Fig. 6. A, the relation of a schematic element of *C. pelagicus* to the calcite cleavage rhomb. B, schematic cross-section through the rhomb showing element profile.

Figs 7–10. AFM of *Helicospaera carteri*. 7, distal shield and blanket. 8, close-up of blanket. 9, proximal view showing base plate scale.

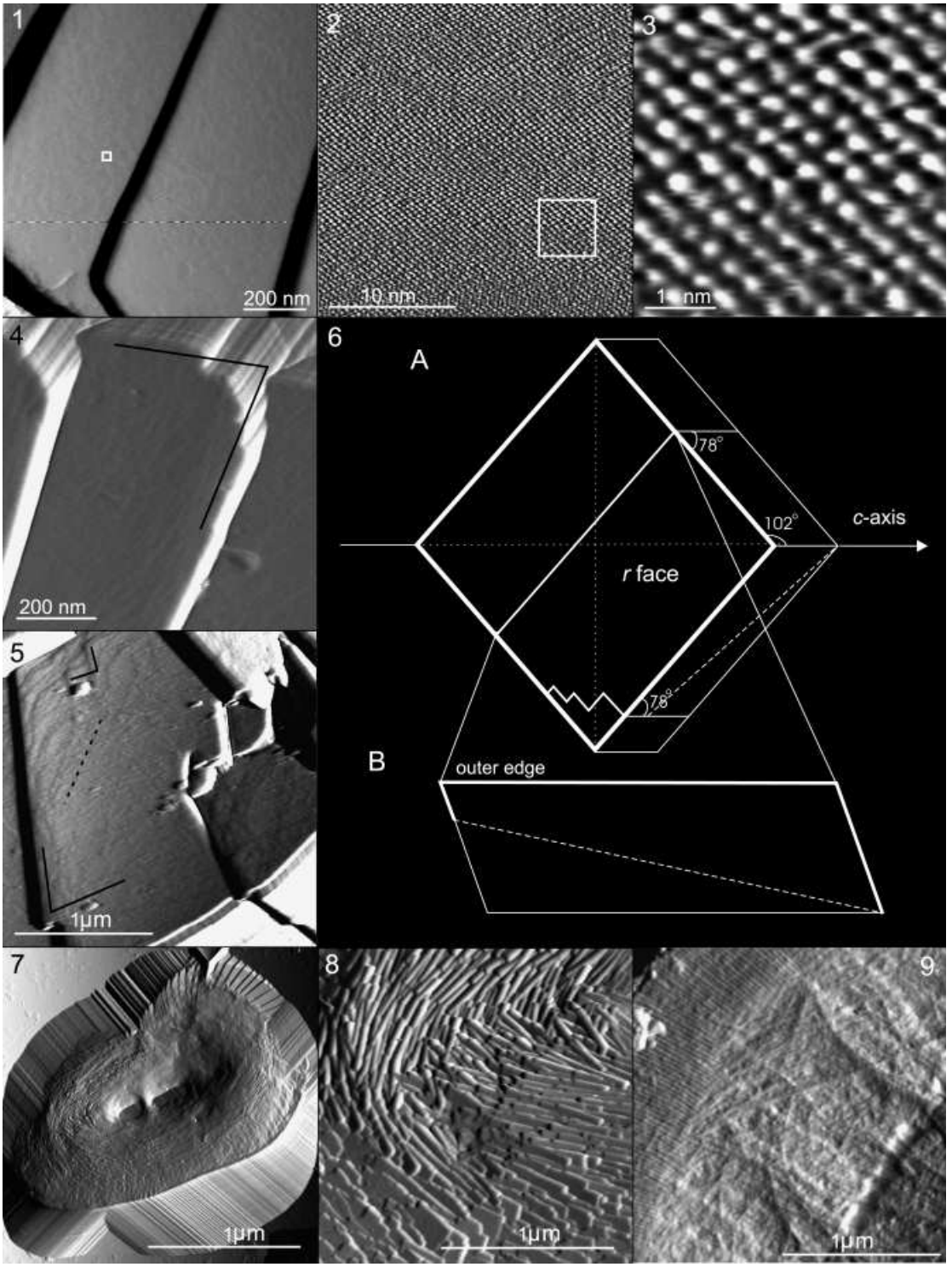

HENRIKSEN *et al.*, coccolith biomineralisation

DISCUSSION

Organic scales

The atomic force microscope resolves organic base-plate scales and body scales excellently. Body scales are commonly observed on the proximal face of *C. pelagicus*, but not on the other two species. The base-plate scales of *H. carteri* underlie the coccolith and have microfibrillar structure on their outer part, whereas the base-plate scale in *C. pelagicus* is without ornament and embedded within the coccolith. SEM results confirm this observation (Pl. 5, fig. 11), which implies that growth occurs around the scale. In *Coccolithus* and *Calcidiscus*, the proto-coccolith belt containing the nucleation sites is not visible on the proximal face, but is located higher up in the structure (Young *et al*. 1992). Therefore, our evidence that the base-plate is distally displaced in *C. pelagicus* is consistent with nucleation occurring on a template attached to this scale, which is believed to be the case for all heterococcoliths (Young *et al*. 1999). In *Coccolithus*, outgrowths from V units form the proximal part of the central area and extensions of the R units form the distal part (Pl. 1, fig. 3); we suggest that the base-plate is located between the two.

Our SEM observations suggest that this is also the case for species of *Umbilicosphaera*, although TEM (transmission electron microscopy) studies of them have indicated that the base-plate underlies the coccoliths (Manton and Leedale 1969; Inouye and Pienaar 1984). This suggests that TEM microtome observations of coccolith-scale relationship need to be assessed carefully, given the problems of coccolith disruption and dissolution during cytological preparation. AFM is clearly a powerful technique for organic scale observations, and consistently supports observations from SEM at lower magnifications, giving confidence in SEM as a tool capable of adding organic scale characters to morphological analyses.

Surface types

AFM demonstrates that the fine-scale morphology of coccolith surfaces is very complex and is a composite of the structure of the calcite and the organic material that drapes across it. Therefore, establishing the structure of the calcite surface is necessary before any definite conclusions can be drawn about the morphology of the coating. Also, establishing calcite morphology is critical in erecting a biomineralisation model, both in terms of revealing the level of complexity that needs to be addressed by the model and by giving hints about the patterns of growth.

Images from oxidised specimens show true calcite morphology and demonstrate that the ultrastructure varies between different parts of the coccoliths: the proximal sides of distal shields have tuberculate textures, whereas distal sides are completely smooth. The surface textures of all untreated specimens are granular, but there is a great variation in texture corrugation, with proximal shields and the underside of distal shields generally being more corrugated than distal surfaces. Aside from the granular textures, fibres have been observed on the distal shield of *O. fragilis* and the proximal shield of *H. carteri*. These long and

---

EXPLANATION OF PLATE 5

Figs 1–2. SEM images of culture material used in this study. 1, *Coccolithus pelagius*. 2, *Oolithotus fragilis*.

Figs 3–5. Tuberculate texture. 3, SEM of *O. fragilis* showing tubercles on the underside of the distal shield. 4, AFM of underside of *O. fragilis* distal shield without organic cover, also showing tubercles. 5, AFM of underside of *C. pelagicus* distal shield. The tubercles are present, although somewhat obscured by the organic cover.

Figs 6–11. SEM of culture material and substrates. 6, granular surface texture that drapes across sutures and is not present on substrates; organic coating. 7, granular surface texture that underlies body scale and must, therefore, be primary. 8–9, granular surface texture present on both sample and substrate, an artefact of preparation. 10, filter substrate only subjected to buffered solution, showing the artefact. 11, proximal view of *C. pelagicus*. The base plate scale enters the coccolith structure.

Fig. 12. SEM of wild sample showing *E. huxleyi* 'collapsed' morphotype (Young 1994), where preferential dissolution has attacked tube elements and element boundaries.

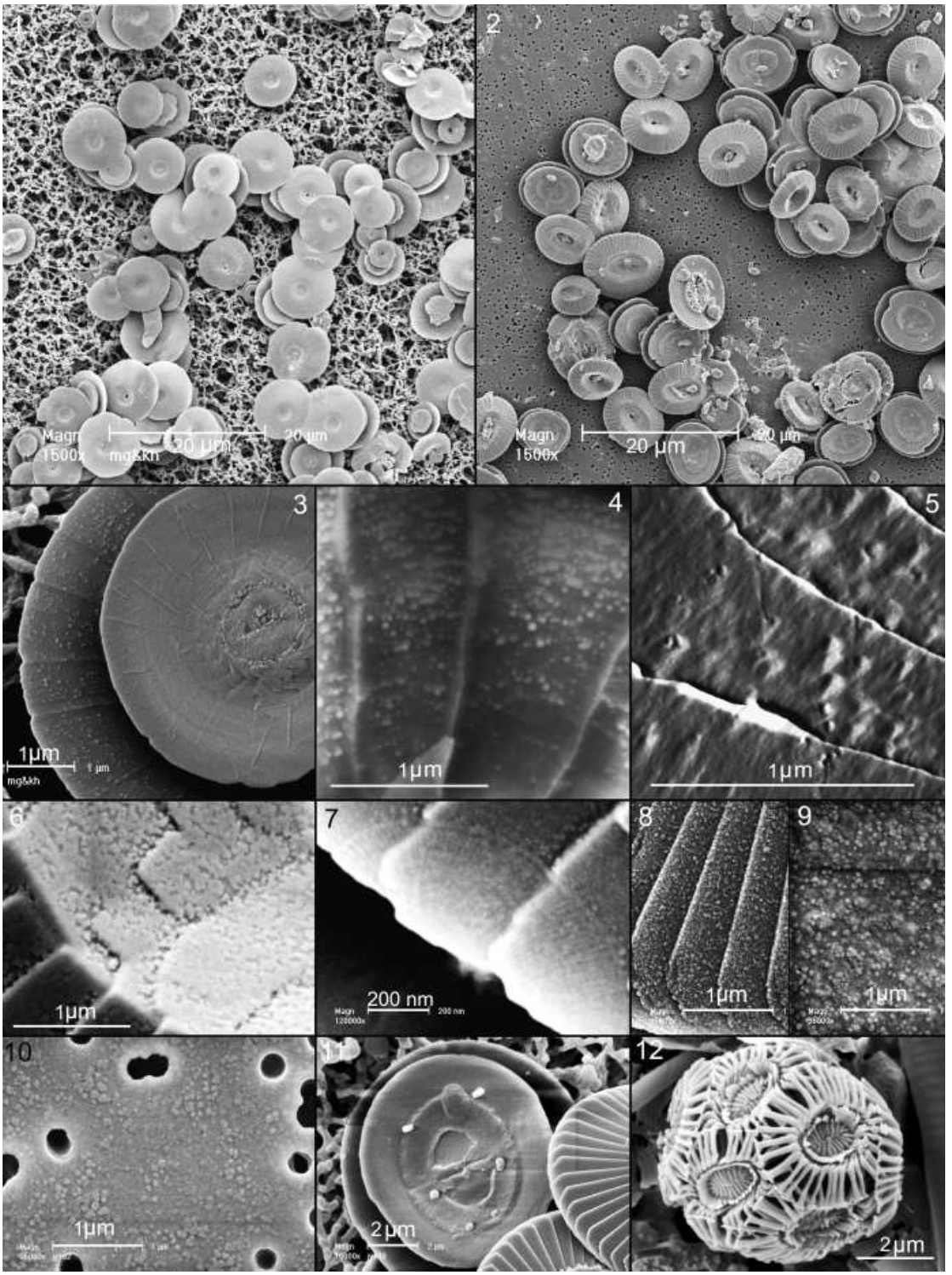

HENRIKSEN *et al.*, coccolith biomineralisation

curving fibres cut across suture lines and bear a remarkable resemblance to the morphology of the polysaccharides extracted from *P. carterae* and imaged with AFM by Smith *et al.* (2000).

The distal face of *O. fragilis* displays a granular cover on the outer part of the shield and fibrous covering inwards from there. Interestingly, these two textures cover calcite of different properties: the granular texture covers the smooth, rhombohedral faces, whereas the fibres overlie the area characterised by numerous steps (Pl. 3, fig. 3). During dissolution, etch pits seem to preferentially form on the areas with fibrous cover; this may be caused by differences in the properties of the calcite (more steps mean higher free energy), or of the organic cover, or both. Therefore, we suggest the term 'surface type' to describe the properties of a calcite surface and its associated organic material, and we can say that the different surface types show variable resistance to dissolution. The different surface types generated during the biomineralisation process are likely to be the result of two-way interactions of organic molecules inducing the formation of different surfaces of calcite, these in turn having properties causing differences in the binding of organic molecules to their faces.

Dissolution behaviour

Separating the two components of a surface type is possible when investigating samples from which the organic coating has been removed by the oxidising treatment. Specimens of *C. pelagicus* subjected to dissolution show that for untreated samples, there is a clear tendency for dissolution to occur at edges and sutures whereas dissolution of treated specimens is concentrated more on the faces. This difference must be caused by the organic coating protecting the faces. Further, dissolution behaviour of treated coccoliths is more regular, i.e. conforms more to the simple rhombic habit of inorganic calcite surfaces than that of untreated specimens where the features are often curved and rounded.

The tendency of dissolution to attack sutures is also evident in wild samples. The 'collapsed' morphotype of *Emiliania huxleyi* (Young 1994) results from etching of specimens at an early stage where their organic cover is presumably intact, and shows preferential dissolution of tube cycles and along element boundaries (Pl. 5, fig. 12). Later diagenetic dissolution of *E. huxleyi* is markedly different and results in etching of shield elements to a larger extent than tube cycles (Burns 1977; Kleijne 1990); we speculate that this is because the organic coating has been removed or damaged by grazing bacteria.

Implications for biomineralisation

The results of our study give clues on some aspects of coccolithogenesis. On *C. pelagicus* and *H. carteri*, growth fronts parallel to the outer edge of elements are common. Step shape and orientation suggest growth upwards and outwards through the addition of layer on layer of calcite. The outer edge of the coccolith is a stable crystallographic direction, meaning its termination is more resistant to mechanical stresses. On *O. fragilis*, this termination is not a cleavage direction and the dominant step direction is not parallel to it.

The models of the crystallographic orientation of distal elements of *C. pelagicus* and *O. fragilis* presented here show marked differences between the two species (Pl. 3, fig. 7; Pl. 4, fig. 6). This is reflected in their morphology. Elements of *O. fragilis* have a curved morphology, whereas those of *C. pelagicus* follow the rhombic structure. The stable rhombic directions are used to construct the straight element edges of *C. pelagicus*, whereas they make the complex zigzag sutures in *O. fragilis*. The termination of *O. fragilis* elements is slightly curved and contains kinks but is overall parallel to the atomic rows, whereas the corresponding surface on *C. pelagicus* is parallel to a cleavage direction. These findings are important because they show us that although nucleation of all heterococcoliths follow the same basic V/R pattern, there are significant differences in the mechanisms operating during subsequent growth.

Morphogenesis of biominerals grown in vesicles is thought to result from two types of influence: cellular stresses that can direct vesicle shape and the action of functional organic molecules that inhibit or accelerate growth (Mann 1983, 1993). Both mechanisms modify patterns of growth so that the morphology of the resulting biomineral is very different from that of its inorganically grown counterpart. For the coccoliths investigated in this study, the different surface types testify to varying degrees of

organic control. Smooth, rhombohedral faces on the proximal sides of distal shields appear to be examples of inorganic growth without surface poisoning, such that growth occurs in layers across the surface. The inner parts of distal shield elements of *O. fragilis* have surfaces dominated by steps that could reflect the modification of inorganic crystal growth by the physical constraints imposed by the vesicle. There is no stabilisation of crystallographic directions that are normally unstable, but merely a termination of growth on cleavage steps; we propose that this occurs once they reach the vesicle wall. Conversely, the proximal surfaces of distal shields are highly modified and appear to have been influenced during growth so material addition is restricted to the leading margin. Tubercles on these surfaces may reflect areas where blockage is imperfect, either by design or by chance. A possible advantage in having them could be that they may strengthen the interlocking of coccoliths in the coccosphere. The contrast between distal and proximal sides of distal shields is puzzling because it indicates that the environments on the two sides of the growing crystals are held quite separate within the laterally expanding vesicle.

CONCLUSIONS

This study shows that atomic force microscopy (AFM) is a useful tool in coccolith biomineralisation research, giving new information about ultrastructure, crystallographic orientation, organic scales and organic coating. As resolved by AFM, the detailed morphology of coccolith calcite is very variable, including smooth crystal faces, surfaces formed from stepped crystal faces, as well as tuberculate surfaces that are not crystallographic faces. The tubercles are part of the calcite structure and located on the underside of distal shields.

AFM under solution allows *in situ* investigation of coccoliths that are dissolving. By conducting these experiments on coccoliths with and without their organic coating, we have demonstrated that the coating protects the faces from etching. This coating is usually either granular or fibrous. On *Oolithotus fragilis*, there seems to be a consistent association of fibrous organic material with the stepped central areas of coccoliths, whereas the outer, flat faces are covered by granular organic material. Because both the organic cover and the calcite surface differ between the two regions, and behaviour during dissolution is influenced by both, we suggest the term ‘surface type’ to distinguish between them.

The organic body scales and base-plate scales of coccolithophores are excellently resolved by AFM, which has proven better than both SEM and TEM at revealing scale-coccolith relationships. The *Helicosphaera carteri* base-plate scale has a microfibrillar structure on its outer part and underlies the coccolith whereas the base-plate scale of *Coccolithus pelagicus* is without ornament and embedded within the coccolith. Because the proto-coccolith nucleation belt is visible on the proximal side of *H. carteri*, but located part way up the structure of *C. pelagicus*, these observations are consistent with nucleation occurring on the base-plate scale in both cases. For *C. pelagicus*, growth occurs upwards, outwards and downwards from the proto-coccolith ring.

We have been able to obtain atomic scale AFM images of *C. pelagicus* and *O. fragilis* distal shield elements, and these enable us to establish their relation to the calcite cleavage rhomb. This evidence reveals marked differences in the biomineralisation of *C. pelagicus* and *O. fragilis*, with *O. fragilis* showing much greater modification of the rhombic calcite motif. Thus, it appears that there are important differences in the mechanisms operating during coccolith growth in different species.

Acknowledgements. We thank Markus Geisen for growing culture samples and helping with SEM; Blair Steel for assisting with culture samples; Ian Probert for providing culture isolates and valuable insights on coccolithophore biology; Dirk Bosbach for supplying the PEI substrate; Birgit Damgaard for help with wet-chemistry lab work; Peter Westbroek for advice on how to remove the organic cover from the coccoliths, and two anonymous referees for valuable comments. Funding was provided by: the Faculty of Science, University of Copenhagen; University College London; the Anglo-Danish Society, and the EU TMR Research Network CODENET (Coccolithophorid Evolutionary Biodiversity and Ecology Network). The SPM laboratory was established through a grant form the Danish Research Council.

REFERENCES

BAUMANN, K. H., YOUNG, J. R., CACHAO, M. and ZIVERI, P. 2000. Biometric study of *Coccolithus pelagicus* and its palaeoenvironmental utility. *Journal of Nannoplankton Research*, **22**, 82.

BILLARD, C. 1994. Life cycles. 167–186. *In* GREEN, J. C. and LEADBEATER, B. S. C. (eds). *The Haptophyte algae*. Systematics Association, Special Volume, **51**, Clarendon Press, Oxford, 446 pp.

BINNING, G., ROHRER, H., GERBER, CH. and WEIBEL, E. 1982*a*. Tunneling through a controllable vacuum gap. *Applied Physics Letters*, **40**, 178–180.

—— —— —— —— 1982*b*. Surface studies by scanning tunneling microscopy. *Physical Review Letters*, **49**, 57–61.

—— QUATE, C. F. and GERBER, C. 1986. Atomic force microscope. *Physical Review Letters*, **56**, 930–933.

BOSBACH, D., CHARLET, L., BICKMORE, B. and HOCHELLA, M. F. 2000. The dissolution of hectorite: *in-situ*, real-time observations using atomic force microscopy. *American Mineralogist*, **85**, 1209–1216.

BRAARUD, T., DEFLANDRE, G., HALLDAL, P. and KAMPTNER, E. 1955. Terminology, nomenclature, and systematics of the Coccolithophoridae. *Micropaleontology*, **1**, 157–159.

BURNS, D. A. 1977. Phenotypes and dissolution morphotypes of the genus *Gephyrocapsa* Kamptner and *Emiliania huxleyi* (Lohmann). *New Zealand Journal of Geology and Geophysics*, **20**, 143–156.

CRAWFORD, S. A., HIGGINS, M. J., MULVANEY, P. and WETHERBEE, R. 2001. Nanostructure of the diatom frustule as revealed by atomic force and scanning electron microscopy. *Journal of Phycology*, **37**, 543–554.

EGGLESTON, C. 1994. High resolution scanning probe microscopy: tip-surface interaction, artifacts, and applications in mineralogy and geochemistry. 3–90. *In* NAGY, K. L. and BLUM, A. E. (eds). *CMS workshop lectures Volume 7: Scanning probe microscopy of clay minerals*. Clay Mineral Society, Boulder, 239 pp.

GEISEN, M., BILLARD, C., BROERSE, A. T. C., CROS, L., PROBERT, I. and YOUNG, J. R. 2002. Life-cycle associations involving pairs of holococcolithophorid species: intraspecific variation or cryptic speciation? *European Journal of Phycology*, **37**, 531–550.

HENRIKSEN, K. and STIPP, S. L. S. 2002. Distortion in scanning probe microscopy. *American Mineralogist*, **87**, 5–17.

—— —— YOUNG, J. R. and BOWN, P. R. 2003. Tailoring calcite: nanoscale AFM of coccolith biocrystals. *American Mineralogist*, **88**, 2040–2044.

INOUYE, I. and PIENAAR, R. N. 1984. New observations on the coccolithophorid *Umbilicosphaera sibogae* var. *foliosa* (Prymnesiophyceae) with reference to cell covering, cell structure and flagellar apparatus. *British Phycological Journal*, **19**, 357–369.

KLEIJNE, A. 1990. Distribution and malformation of extant calcareous nannoplankton in the Indonesian seas. *Marine Micropalaeontology*, **16**, 293–316.

—— 1993. Morphology, taxonomy and distribution of extant coccolithophorids (calcareous nannoplankton). PhD thesis, Free University Amsterdam, 321pp.

MANN, S. 1983. Mineralization in biological systems. *Structure and Bonding*, **54**, 125–174.

—— 1993. Molecular tectonics in biomineralization and biomimetic materials chemistry. *Nature*, **365**, 499–505.

MANTON, I. and LEEDALE, G. F. 1969. Observations on the microanatomy of *Coccolithus pelagicus* and *Cricosphaera carterae*, with special reference to the origin and nature of coccoliths and scales. *Journal of the Marine Biological Association of the UK*, **49**, 1–16.

MARSH, M. E. 1994. Polyanion-mediated mineralization – assembly and reorganization of acidic polysaccharides in the golgi system of a coccolithophorid alga during mineral deposition. *Protoplasma*, **177**, 108–122.

OHNESORGE, F. and BINNIG, G. 1993. True atomic-resolution by atomic force microscopy through repulsive and attractive forces. *Science*, **260**, 1451–1456.

ORME, C. A., NOY, A., WIERSZBICKI, A., MCBRIDE, M. T., GRANTHAM, M., TENG, H. H., DOVE, P. M. and DEYOREO, J. J. 2001. Formation of chiral morphologies through selective binding of amino acids to calcite surface steps. *Nature*, **411**, 775–779.

OUTKA, D. E. and WILLIAMS, D. C. 1971. Sequential coccolith morphogenesis in *Hymenomonas carterae*. *Journal of Protozoology*, **18**, 285–297.

SMITH, B. L., PALOCZI, G. T., HANSMA, P. K. and LEVINE, R. P. 2000. Discerning nature's mechanism for making complex biocomposite crystals. *Journal of Crystal Growth*, **211**, 116–121.

STIPP, S. L. S. 1999. Toward a conceptual model of the calcite surface: hydration, hydrolysis, and surface potential. *Geochemica et Cosmochemica Acta*, **63**, 3121–3131.

—— EGGLESTON, C. M. and NIELSEN, B. S. 1994. Calcite surface structure observed at microtopographic and molecular scales with atomic force microscopy (AFM). *Geochimica et Cosmochimica Acta*, **58**, 3023–3033.

—— GUTMANNSBAUER, W. and LEHMAN, T. 1996. The dynamic nature of calcite surfaces in air. *American Mineralogist*, **81**, 1–8.

THEODORIDIS, S. 1984. Calcareous nannofossil biozonation of the miocene and revision of the helicoliths and discoasters. *Utrecht Micropaleontological Bulletins*, **32**, 271 pp.

VAN DER WAL, P., DE JONG, E. W., WESTBROEK, P., BRUIJN, W. C. and MULDER-STAPEL, A. A. 1983. Polysaccharide localization, coccolith formation and golgi dynamics in the coccolithophorid *Hymenomonas carterae*. *Journal of Ultrastucture Research*, **85**, 139–158.

YOUNG, J. R. 1993. The description and analysis of coccolith structure. *Knihovnicka ZPN*, **14a**, 35–71.

—— 1994. Variation in *Emiliania huxleyi* coccolith morphology in samples from the norwegian Ehux experiment, 1992. *Sarsia*, **79**, 427–425.

—— and HENRIKSEN, K. 2003. Biomineralization within vesicles: the calcite of coccoliths. 189–215. *In* DEVE, P., DE YOREO, J. J. and WEINER, S. (eds). *Biomineralization*. Reviews in Mineralogy and Geochemistry, **56**, 381 pp.

—— DAVIS, S. A., BOWN, P. R. and MANN, S. 1999. Coccolith ultrastructure and biomineralisation. *Journal of Structural Biology*, **126**, 195–215.

—— DIDYMUS, J. M., BOWN, P. R., PRINS, B. and MANN, S. 1992. Crystal assembly and phylogenetic evolution in heterococcoliths. *Nature*, **356**, 616–618.

K. HENRIKSEN

S. L. S. STIPP

NanoGeoScience
Geological Institute
University of Copenhagen
Øster Voldgade 10
Dk-1350 København K, Denmark
e-mail k.henriksen@geo.geol.ku.dk

J. R. YOUNG

Palaeontology Department
The Natural History Museum
Cromwell Road
London SW7 5BD, UK

P. R. BOWN

Postgraduate Unit of Micropalaeontology
Department of Geological Sciences
University College London
Gower Street
London WC1E 6BT, UK

Typescript received 10 October 2002
Revised typescript received 26 February 2003